This document presents supplementary data and methods to support a separate manuscript currently in review at the JOURNAL OF GEOPHYSICAL RESEARCH. The large volume of data tables, static images, and videos presented herein are beyond the scope for publication in JGR but are nonetheless useful to disclose all model results, including model failures, to interested parties. If the JGR paper is accepted for publication, it will be linked to this EARTHARXIV methods and results paper.

Please contact any of the authors on the content presented herein; we welcome constructive feedback.

An investigation of multi-fault rupture scenarios using a variety of Coulomb stress modelling criteria: methods paper and full results

Mark Quigley

School of Earth Sciences, The University of Melbourne, Victoria 3010, Australia
Mark.quigley@unimelb.edu.au
https://orcid.org/0000-0002-4430-4212

Abigail Jiménez Lloret

Department of Computer science and artificial intelligence, Universidad de Granada, 51001 Ceuta, Spain
ajlloret@ual.es

Brendan Duffy

School of Earth Sciences, The University of Melbourne, Victoria 3010, Australia
brendan.duffy@unimelb.edu.au
https://orcid.org/0000-0001-6638-5108

Tamarah King

School of Earth Sciences, The University of Melbourne, Victoria 3010, Australia
tamarah.king@unimelb.edu.au
https://orcid.org/0000-0002-9654-2917

Abstract

A series of Coulomb stress models are used to simulate the independently-derived (Holden et al., 2011) rupture process of Mw 7.1 Darfield earthquake. The 7-fault source model of Beavan et al. (2012) is used for all models. Model differences include (i) differences in the static stress thresholds (0,1,5,10 MPa) that must be reached or exceeded to initiate rupture on a receiver fault, (ii) differences in whether fault-averaged, fault summative total, or maximum values of static stress on receiver faults are used with different threshold values from (i) to evaluate whether rupture proceeds or not, and (iii) whether rupture initiates only on the fault with the maximum static stress value (i.e., hierarchical model) or whether multiple faults where the static stress exceeds the threshold value can rupture concurrently (i.e., stress threshold model). Maximum static stress models in the stress threshold family with thresholds of 1 and 5 MPa most successfully replicate the Holden et al. (2011) Darfield rupture sequence, although further model modifications to thresholds based on fault slip tendency analyses, presented in Quigley et al. (in review), improve the consistency between model observations and the Holden et al. (2011) hypothesis.

Introduction

Recent earthquake events such as the 2016 Mw 7.8 Kaikoura earthquake (New Zealand) (Hamling et al., 2017; Litchfield et al., 2018) and 2010 Mw 7.2 El Mayor-Cucapah earthquake (Mexico) (Fletcher et al., 2016; Wei et al., 2011) demonstrate the complex nature of earthquake events in interlinked multi-fault systems. Modelling rupture scenarios and potential maximum magnitude events in multi-fault systems has significant implications for hazard modelling and characterisation (Field et al., 2014). Recent work has used Coloumb stress change (CSC) analysis to investigate multi-fault earthquake scenarios, including multi-fault rupture cascades (Fletcher et al., 2016) and spatio-temporally clustered earthquakes (Walters et al., 2018).

We present a methodology for CSC based multi-fault rupture modelling using the 2010 Mw 7.1 Darfield earthquake event in New Zealand as an example. Our methods are similar to CSC multi-rupture modelling undertaken by Parsons et al. (2012) and Fletcher et al. (2016).

We present a full suite of results from our CSC modelling methodology in this paper, which are discussed in further detail in a submitted manuscript to the JOURNAL OF GEOPHYSICAL RESEARCH. The submitted manuscript combines the results included in this EARTHARXIV paper with additional analysis of empirically derived stress drop estimates, Mohr-Coulomb fault slip tendency and Gutenberg-Richter scaling and b-value estimates for the Darfield earthquake.

The Canterbury earthquake sequence (Quigley et al., 2016) started with the Darfield rupture on 2010 September 3 with a Mw 7.1 earthquake. This event is interpreted to have ruptured at least six reverse and strike slip faults or fault segments (Beavan et al., 2012; Elliott et al., 2012). Analysis of the Darfield rupture sequence suggests that the hypocentral source fault of initial rupture is the Charing Cross reverse fault (CCF) (Beavan et al., 2012; Gledhill et al., 2010) which then propagated onto neighbouring faults including the Charing Cross north fault (CCn), Greendale central fault (GFc), Greendale east fault (GFe) Sandy Knolls fault (SKF), and Hororata Anticline fault (HAF) (Fig. 1). Holden et al. (2011) present a rupture order model, with rupture propagating from the CCF hypocentre in a SW direction towards to the Greendale fault (GF), NW onto the Charing Cross north fault (CCFn), eastward onto the central section of the Greendale fault (GFc), toward the Sandy Knolls blind oblique-reverse fault (SKF) and Greendale fault east (GFe), and westward on to the Greendale fault west (GFw), toward the Hororata Anticline Fault (HAF).

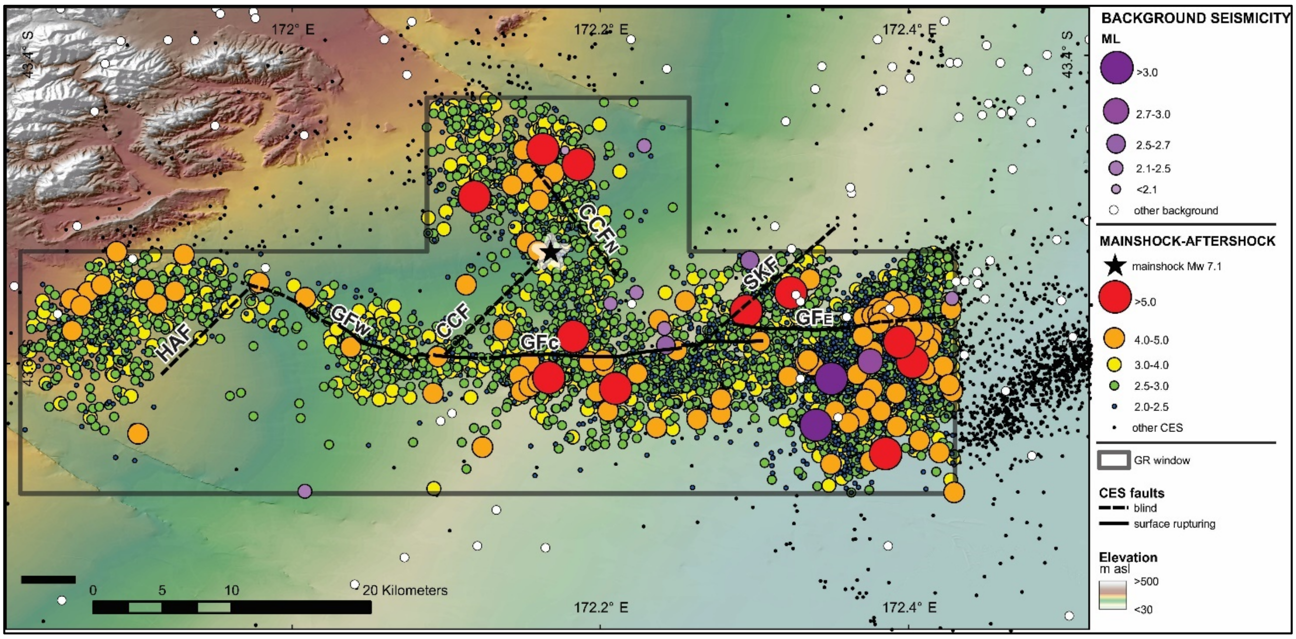

Fig. 1 Darfield earthquake source faults based on Beavan et al. (2010)

We aim to investigate different Coulomb stress change modelling approaches to replicate the published rupture order of Holden et al. (2011) and observe how rupture may have propagated if the hypocentral fault were any other in the system. We present our methodology and all results in static image, video and excel format.

Method

We use standard methodology for Coulomb stress modelling (King et al., 1994) to calculate static stress changes imposed by source fault ruptures (hypocentral fault) onto proximal receiver faults using Okada's (1992) equations.

We apply a branching model network to investigate variations in multi-fault ruptures depending on hypocentral fault location and CSC based criteria to investigate how stress changes affect multi-fault rupture in different scenarios (Fig 2). We use the fault source model presented in Beavan et al (2012) and run models first with the CCF as hypocentral fault, and then where rupture initiates on any other fault in the system (Fig. 1).

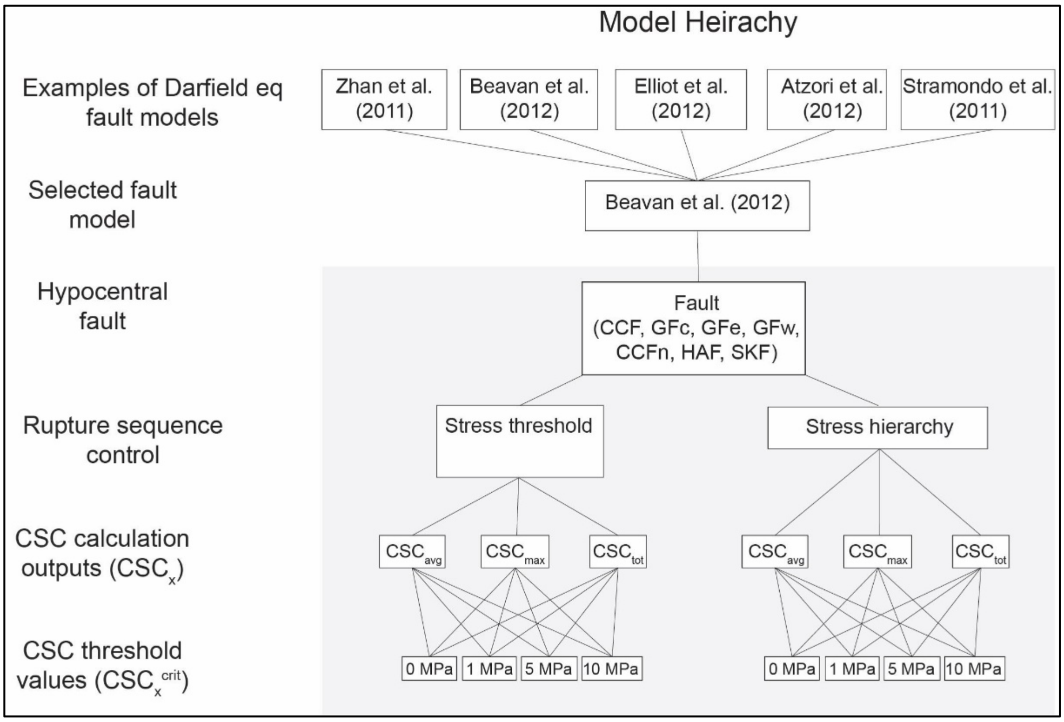

Fig 2. Flow chart showing branching model network with all model steps and CSC based criteria. The model steps are repeated for all hypocentral faults, resulting in 168 individual model outcomes.

The two branches of models follow two analytical approaches for Rupture Sequence Control (Fig. 2, Fig 3.). The first, "Stress threshold", assumes instantaneous rupture occurs on any receiver fault if the imposed CSC is greater than the defined critical CSC value (CSC^{crit}), with recalculation of stress on un-ruptured receiver faults. The second approach, "stress hierarchy" assumes only the receiver fault with the highest CSC value ruptures, and CSC values are then recalculated across the remaining receiver faults. Rupture ceases in both approaches when the imposed CSC on a receiver fault is < CSC^{crit}. The stress hierarchy approach has similar theoretical aspects to the rupture branching analysis conducted by Parsons et al. (2012).

Three sets of "CSC calculation outputs" are then modelled (Fig 2.): the average of the CSC values (CSC_{ave}); the maximum CSC value (CSC_{max}); and the total sum of CSC values (CSC_{tot}) (Fig 4). These determine how the static stress changes for each 1km^2 receiver fault pixel are calculated to determine whether the applied critical CSC value (CSC^{crit}) has been exceeded for fault rupture to occur (Fig 3). The CSC^{crit} values applied for each model are 0 MPa, 1 MPa, 5 MPa, and 10 MPa.

The total number of models is therefore 168 with branches of: 7 x Rupture Order (CCF first based on Holden et al. (2011), or initiation on any of the other 6 faults); 2 x Rupture Sequence Control (stress threshold and stress hierarchy); 3 x CSC Calculation Outputs (CSC_{ave}, CSC_{max}, CSC_{tot}); and 4x CSC Thresholds (0 MPa, 1 MPa, 5 MPa, and 10 MPa).

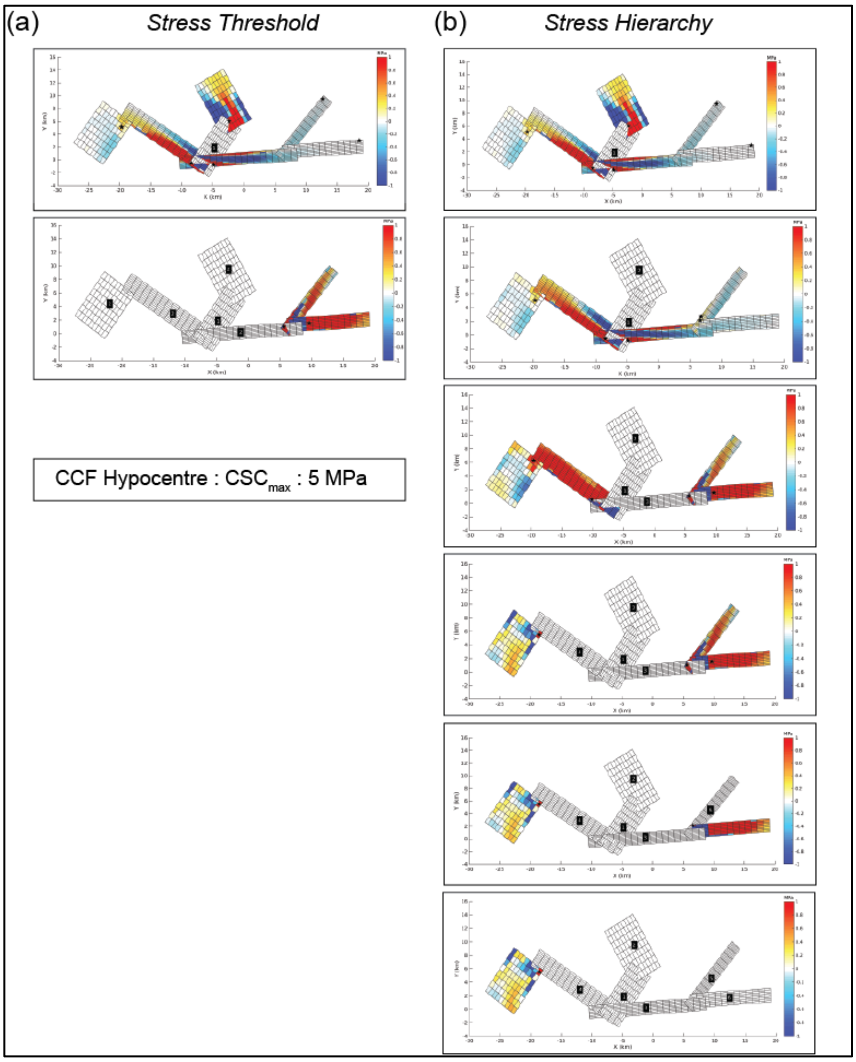

Fig 3. Example of "stress threshold" and "stress hierarchy" Rupture Sequence Control results demonstrating (a) four receiver faults receiving $CSC_{max} \geq 5$ MPa and simultaneously rupturing, with subsequent recalculation of stress on other receiver faults, until no faults have $CSC_{max} \geq 5$ MPa (b) a single receiver fault with the highest CSC_{max} rupturing with subsequent recalculation of stress on all receiver faults in a recurrent fashion until no faults have $CSC_{max} \geq 5$ MPa

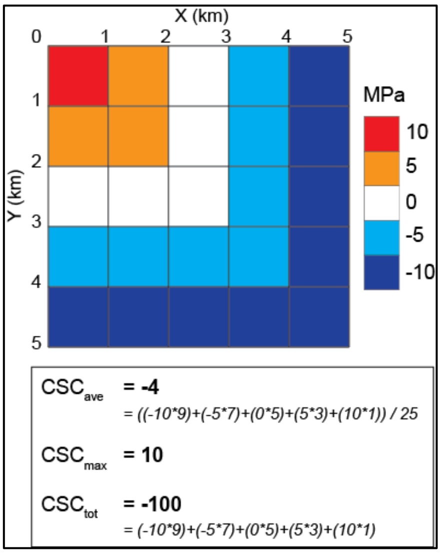

Fig 4. Visualisation of "CSC Calculation Outputs" for a fault plane with example coulomb static stress changes

Summary of results

CSC modelling results are presented in two excel workbooks included with this paper. The first file includes results for all "Stress Threshold" models, and the other all "Stress hierarchy". Each excel workbook contains three sheets (tabs), documenting results for CSC_{ave}, CSC_{max}, and CSC_{tot}. Each sheet documents initiation of rupture on each of the seven faults, and demonstrates the number of steps required for either (i) all faults to rupture or (ii) rupture termination based on CSC threshold values of 0, 1, 5, 10 MPa.

All the results included in the excel worksheets are shown visually as static images with the naming structure:

Rupture sequence control	CSC calculation output	CSC threshold value	Hypocentral fault	Step number
"Darfield" = stress threshold "Darfield_Parsons" = stress hierarchy	CSCavg = avgstress CSCmax = maxstress CSCtot = totstress	0, 1, 5, 10 MPa	1 – GFc 2 – GFw 3 – Gfe 4 – CCF 5 – HAF 6 – CCFn 7 - SKF	1 – 7 The final step (i.e. all faults ruptured) is not included in the static images, or videos.

Table 1: naming structure for static images included in supplement, with each step separated by an underscore.

For example *"Darfield_avestress_0MPa_1_1.jpg"* is the first rupture step with the GFc as hypocentral fault, under the stress threshold model, with CSC_{avg}^{crit} = 0 MPa.

All models are included as video files demonstrating the complete steps required to either (i) rupture all faults or (ii) terminate rupture. Two video files show the CCF as the hypocentral fault with all CSC calculation outputs and CSC thresholds for the "stress threshold" Rupture Sequence Control, followed by all models under the "stress hierarchy" Rupture Sequence Control. Six videos the show results for all CSC thresholds (0 MPa, 1 MPa, 5 MPa, and 10 MPa) for all seven potential hypocentral fault scenarios (Fig 1.) with variables of CSC Calculation Outputs and Rupture Sequence Controls (i.e. 3x Stress Hierarchy videos for CSC_{ave}, CSC_{max}, $CSC_{tot;}$ 3x Stress Threshold videos for CSC_{ave}, CSC_{max}, CSC_{tot}).

Figure 5 summarises the full results by demonstrating the number of steps required for the model to either (i) rupture all faults (n = 32) or (ii) terminate rupture (n = 136). Green stars indicate what models ruptured all faults, rather than terminating because no faults in the step had CSC values greater than the defined CSC_x^{crit} value. Red stars indicate models that terminated prior to rupturing all faults.

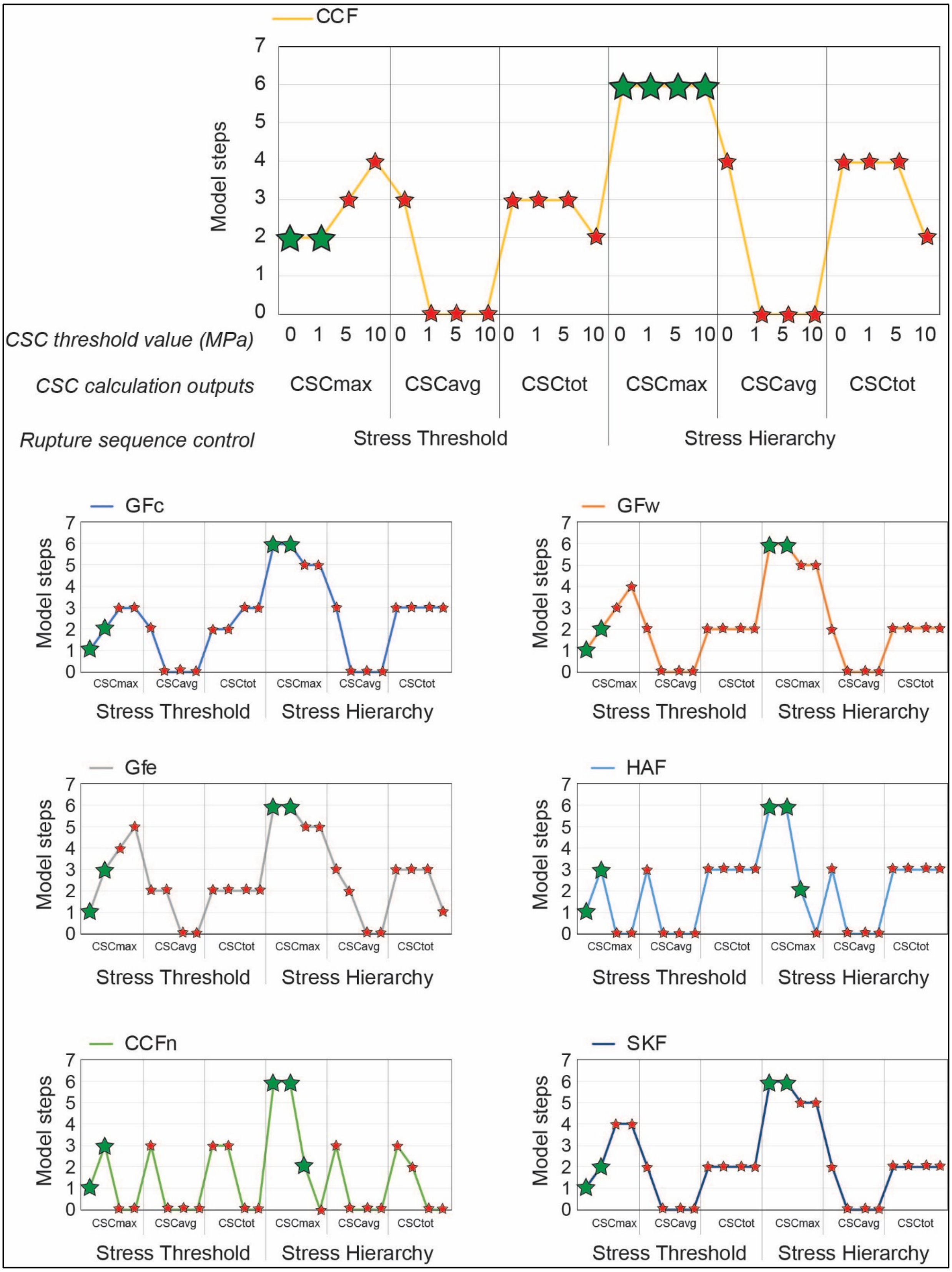

Fig 5. Graphs demonstrating the number of steps required to either rupture all faults or terminate rupture for each hypocentral fault initiation. The top graph includes all labels for all branches of CSC model criteria, for reference with the other graphs. Green stars indicate which models completely ruptured all faults (i.e. all faults experienced $CSC_x \geq CSC_x^{crit}$), red stars indicate models that terminate when no more faults fit the criteria (i.e. $CSC_x \leq CSC_x^{crit}$)

Discussion points

The results (excel workbooks, static images, videos and graphs) show which branches of our CSC model criteria were most successful at replicating the Holden et al. (2011) rupture scenario for the Darfield earthquake (initiation on CCF), and also explore how the multi-fault system may behave if rupture initiates on any of the other faults in the system.

Figure 5 shows that models with CSC_{max}^{crit} values of 0 and 1 MPa were the most successful at rupturing all faults, in both the Stress Threshold and Stress Hierarchy systems. None of the CSC_{avg} or CSC_{tot} models were successful at rupturing all faults, with models ceasing rupture most commonly within 2 steps after no faults reached the CSC_{x}^{crit} value. The sequence of faults ruptured for each all of these scenarios changes depending on the hypocentral fault (this data is available in the excel spreadsheets, static images and videos).

Our modelling aims to address a variety of questions including:

- Is the sequence of fault rupture and duration (i.e. rupture steps before termination) of multi-fault rupture affected by different methods to calculate when CSC^{crit} has been overcome for an individual receiver fault (i.e. CSC_{ave}, CSC_{max}, CSC_{tot});
- How do geologically reasonable CSC^{crit} values for fault rupture (i.e. 1 MPa for optimally orientated faults and 5 MPa for misorientated faults) compare to a minimum value (0 MPa) and a maximum value (10 MPa) on how many receiver faults will rupture in an event, and how many steps to termination of rupture;
- What method of rupture sequence control (stress threshold or stress hierarchy) best simulates a known multi-fault rupture event (i.e. the Darfield earthquake sequence);
- How is rupture sequence and duration affected by initiation on different faults in a multi-fault system, and what variety of CSC-modelling best describes (i) a known rupture and (ii) previously published explanations for multi-fault rupture (i.e. the Keystone Fault model of Fletcher et al. (2016)).

These results are explored in more detail in our submitted manuscript to JOUNRAL OF GEOPHYSICAL RESEARCH and are combined with analysis of other seismological and geological data to explore controls on multi-fault system rupture behaviour, maximum potential magnitude, and frequency-magnitude distributions.

References

Beavan, J., Motagh, M., Fielding, E.J., Donnelly, N., Collett, D., 2012. Fault slip models of the 2010-2011 Canterbury, New Zealand, earthquakes from geodetic data and observations of postseismic ground deformation. New Zeal. J. Geol. Geophys. 55, 207–221. https://doi.org/10.1080/00288306.2012.697472

Elliott, J.R., Nissen, E.K., England, P.C., Jackson, J.A., Lamb, S., Li, Z., Oehlers, M., Parsons, B., 2012. Slip in the 2010-2011 Canterbury earthquakes, New Zealand. J. Geophys. Res. Solid Earth 117. https://doi.org/10.1029/2011JB008868

Field, E.H., Arrowsmith, R.J., Biasi, G.P., Bird, P., Dawson, T.E., Felzer, K.R., Jackson, D.D., Johnson, K.M., Jordan, T.H., Madden, C., Michael, A.J., Milner, K.R., Page, M.T., Parsons, T., Powers, P.M., Shaw, B.E., Thatcher, W.R., Weldon, R.J., Zeng, Y., 2014. Uniform California Earthquake Rupture Forecast, version 3 (UCERF3) -The time-independent model. Bull. Seismol. Soc. Am. 104, 1122–1180. https://doi.org/10.1785/0120130164

Fletcher, J.M., Oskin, M.E., Teran, O.J., 2016. The role of a keystone fault in triggering the complex El Mayor-Cucapah earthquake rupture. Nat. Geosci. 9, 303–307. https://doi.org/10.1038/ngeo2660

Gledhill, K., Ristau, J., Reyners, M., Fry, B., Holden, C., 2010. The Darfield (Canterbury, New Zealand) Mw 7.1 earthquake of September 2010: A preliminary seismological report. Bull. New Zeal. Soc. Earthq. Eng. 43, 215–221. https://doi.org/10.1785/gssrl.82.3.378

Hamling, I.J., Hreinsdóttir, S., Clark, K., Elliott, J., Liang, C., Fielding, E., Litchfield, N., Villamor, P., Wallace, L., Wright, T.J., D'Anastasio, E., Bannister, S., Burbidge, D., Denys, P., Gentle, P., Howarth, J., Mueller, C., Palmer, N., Pearson, C., Power, W., Barnes, P., Barrell, D.J.A., Van Dissen, R., Langridge, R., Little, T., Nicol, A., Pettinga, J., Rowland, J., Stirling, M., 2017. Complex multifault rupture during the 2016 Mw7.8 Kaikōura earthquake, New Zealand. Science (80-.). 356. https://doi.org/10.1126/science.aam7194

Holden, C., Beavan, J., Fry, B., Reyners, M., Ristau, J., Dissen, R. Van, Villamor, P., Quigley, M., 2011. Preliminary source model of the Mw 7.1 Darfield earthquake from geological, geodetic and seismic data, in: Proceedings of the Ninth Pacific Conference on Earthquake Engineering Building an Earthquake-Resilient Society 14-16 April, 2011. Auckland, New Zealand. https://doi.org/10.2165/00002018-199410020-00003

King, G.C.P., Stein, R.S., Lin, J., 1994. Static stress changes and the triggering of earthquakes. Bull. Seismol. Soc. Am. 84, 935–953. https://doi.org/10.1016/0148-9062(95)94484-2

Litchfield, N.J., Villamor, P., van Dissen, R.J., Nicol, A., Barnes, P.M., Barrell, D.J.A., Pettinga, J.R., Langridge, R.M., Little, T.A., Mountjoy, J.J., Ries, W.F., Rowland, J., Fenton, C., Stirling, M.W., Kearse, J., Berryman, K.R., Cochran, U.A., Clark, K.J., Hemphill-Haley, M., Khajavi, N., Jones, K.E., Archibald, G., Upton, P., Asher, C., Benson, A., Cox, S.C., Gasston, C., Hale, D., Hall, B., Hatem, A.E., Heron, D.W., Howarth, J., Kane, T.J., Lamarche, G., Lawson, S., Lukovic, B., McColl, S.T., Madugo, C., Manousakis, J., Noble, D., Pedley, K., Sauer, K., Stahl, T., Strong, D.T., Townsend, D.B., Toy, V., Williams, J., Woelz, S., Zinke, R., 2018. Surface rupture of multiple crustal faults in the 2016 Mw7.8 Kaikōura, New Zealand, earthquake. Bull. Seismol. Soc. Am. 108, 1496–1520. https://doi.org/10.1785/0120170300

Okada, Y., 1992. Internal deformation due to shear and tensile faults in a half-space. Bull. Seismol. Soc. Am. 82, 1018–1040. https://doi.org/10.1.1.484.8168

Parsons, T., Field, E.H., Page, M.T., Milner, K., 2012. Possible earthquake rupture connections on mapped California faults ranked by calculated Coulomb linking stresses. Bull. Seismol. Soc. Am. 102, 2667–2676. https://doi.org/10.1785/0120110349

Quigley, M., Hughes, M., Bradley, B., van Ballegooy, S., Reid, C., Morgenroth, J., Horton, T., Duffy, B., Pettinga, J. (2016) The 2010-2011 Canterbury earthquake sequence: environmental effects, seismic triggering thresholds, and geologic legacy, Tectonophysics, doi: 10.1016/j.tecto.2016.01.044

Walters, R.J., Gregory, L.C., Wedmore, L.N.J., Craig, T.J., McCaffrey, K., Wilkinson, M., Chen, J., Li, Z., Elliott, J.R., Goodall, H., Iezzi, F., Livio, F., Michetti, A.M., Roberts, G., Vittori, E., 2018. Dual control of fault intersections on stop-start rupture in the 2016 Central Italy seismic sequence. Earth Planet. Sci. Lett. 500, 1–14. https://doi.org/10.1016/j.epsl.2018.07.043

Wei, S., Fielding, E., Leprince, S., Sladen, A., Avouac, J.P., Helmberger, D., Hauksson, E., Chu, R., Simons, M., Hudnut, K., Herring, T., Briggs, R., 2011. Superficial simplicity of the 2010 El Mayorg-Cucapah earthquake of Baja California in Mexico. Nat. Geosci. 4, 615–618. https://doi.org/10.1038/ngeo1213